Carbohydrate Polymers 80 (2010) 695–698

Contents lists available at ScienceDirect

Carbohydrate Polymers

journal homepage: www.elsevier.com/locate/carbpol

A synthetic macromolecule as MRI detectable drug carriers: Aminodextran-coated iron oxide nanoparticles

Mohammad Reza Saboktakin [a,*], Roya M. Tabatabaie [a], Abel Maharramov [b], Mohammad Ali Ramazanov [b]

[a] Nanostructured Materials Synthesis Lab., International Research Institute of Arian Chemie Gostar, Tabriz, Iran
[b] Nanotechnology Research Center, Baku State University, Baku, Azerbaijan

ARTICLE INFO

Article history:
Received 24 October 2009
Received in revised form 26 November 2009
Accepted 30 November 2009
Available online 16 December 2009

Keywords:
Macromolecule
MRI
Aminodextran
Iron oxide nanoparticles
Drug carriers

ABSTRACT

A new synthetic macromolecule, aminodextran-coated iron oxide nanoparticles, was synthesized as drug carrier detectable using magnetic resonance imaging (MRI) technique. The synthesis process starts with a 2-step reaction that attaches a high density of amino groups to a dextran backbone. These macromolecules were coated with magnetic iron oxide molecules by a chemical reaction that can carry several molecules such as drug and peptides. The aminodextran-coated iron oxide nanoparticles thus synthesized have been characterized by Fourier infrared (FT-IR) spectroscopy. Also, the morphology of this synthetic macromolecule was studied by scanning electron microscopy.

1. Introduction

Nanomedicine is an emerging field that uses nanoparticles to facilitate the diagnosis and treatment of diseases. Notable early successes in the clinic include the use of magnetic nanoparticles as a contrast agent in MRI and nanoparticle-based treatment systems (Vera, Buonocore, Wisner, Katzberg, & Stadalnik, 1995). The first generation of nanoparticles used in tumor treatments rely on leakiness of tumor vessels for preferential accumulation in tumor; however, this enhanced permeability and retention is not a constant feature of tumor vessels and even when present, still leaves the nanoparticles to negotiate the high interstitial fluid pressure in tumors (Morton, Wen, & Wong, 1992; Vera, Wisner, & Stadalnik, 1997). An attractive alternative would be to target nanoparticles to specific molecular receptors in the blood vessels because they are readily available for binding from the blood stream and because tumor vessels express a wealth of molecules that are not significantly expressed in the vessels of normal tissues (Gershenwald, Tseng, & Thomson, 1998; Glass, Messina, & Cruse, 1996).

Specific targeting of nanoparticles to tumors has been accomplished in various experimental systems (Giuliano, Kirgan, Guenther, & Morton, 1994), but the efficiency of delivery is generally low. An amplified homing is an important mechanism that ensures sufficient platelet accumulation at the sites of vascular injury (Chipowsky & Lee, 1973; Lee, Stowell, & Krantz, 1976). Amplified homing involves target binding, activation, platelet–platelet binding, and formation of a blood clot. Nanoparticle-based diagnostics and therapeutics hold great promise because multiple functions can be built into the particles (Qu, Wang, Zhu, Rusckowski, & Hnatowich, 2001; Shirakami et al., 1987). One such function is an ability to home to specific sites in the body. A research describe the magnetic particles new application not only home to tumors, but also amplify own homing (Porter, 1997; Tomalia, Baker, & Deward, 1985). The system is based on a magnetic drug–dextran conjugate that carries anti-tumor drug molecules (Nugent & Jain, 1984; Thoren, 1978). Iron oxide nanoparticles coated with this dextran–drug conjugate thereby producing new binding sites for more particles (Korosy & Barczai-Martos, 1950; Krejcarek & Tucker, 1977). A nanoparticle delivery system has been designed in which the particles amplify their own homing in a manner that resembles platelet (de Belder, 1996).

2. Materials and methods

2.1. Materials

Pharmaceutical-grade dextran (PM70, weight average molecular weight, 70,000) was obtained from Baku State University. All aqueous solutions were prepared using deionized water (NANO pure) infinity, Barnstead/Thermolyne, Dubuque, IA).

Dimethylsulfoxide, ammonium persulfate and methanol were obtained from Aldrich Chemicals. All dextran conjugates were

* Corresponding author. Tel./fax: +98 4116694803.
E-mail address: saboktakin123@yahoo.com (M.R. Saboktakin).

0144-8617/$ - see front matter © 2009 Elsevier Ltd. All rights reserved.
doi:10.1016/j.carbpol.2009.11.051

lyophilized and stored at −80 °C. Dextran standards (stored at −80 °C) were prepared by dissolution in deionized water followed by lyophilization. All other reagents were purchased from commercial suppliers and used as received.

2.2. Methods

2.2.1. Synthesis of allyl-dextran (PM70)

PM70 dextran (10 g) in 75 mL deionized water was prepared at 50 °C and pH 11 in the presence of 2.5 g sodium hydroxide and 0.2 g sodium borohydride. The pH was maintained by dropwise addition of 2.5N NaOH and 2 mL allyl bromide. The solution was neutralized with acetic acid (2.5 mol/L) and the reaction mixture was placed in a 5 °C refrigerator for 2 h. After the top organic layer was decanted and 100 mL deionized water was added, the resulting solution was filtered (5 μm) into an ultrafiltration cell and diafiltered (molecular weight cut off, 3000) with 10 exchange volumes of deionized water. The product, allyl-dextran, was then concentrated and lyophilized.

2.2.2. Synthesis of aminodextran conjugate

The allyl-dextran was reacted with 7.5 g aminoalkyl thiol compound in 30 mL dimethylsulfoxide to produce an aminodextran conjugate. This reaction was initiated with 0.1 g ammonium persulfate and was performed under a nitrogen atmosphere. The volume of the reaction mixture after 3 h was doubled with deionized water, then, the solution was adjusted to pH 4 with sodium hydroxide (2.5N), and the product was diluted with 140 mL sodium acetate buffer (0.02 mol/L, pH 4). The product was then filtered (5 μm) into an ultrafiltration cell and dialyzed with five exchange volumes of deionized water. After concentration, the aminodextran conjugate was lyophilized. A sample was then assayed for the average number of amino groups per dextran, which was defined as the amine density.

2.2.3. Synthesis of aminodextran-coated iron oxide nanoparticles

Aminodextran conjugate (0.5 g) and 35 mg $FeCl_3{\cdot}6H_2O$ were solved in 4 mL H_2O and nitrogen was flushed for 1.5 h. $FeCl_2{\cdot}4H_2O$ (14 mg) was added, followed by 100 μL aqueous ammonia in two portions while the mixture was kept under nitrogen. The solution turned black and was heated to 80 °C for 100 min. After the mixture was cooled to room temperature, the ammonia was removed by flushing the solution with nitrogen over 10 min. Freeze drying led to the desired particles (0.55 mg), which are stable at 4 °C for at least 1 year and were used for all further experiments. Titration of the resulting particle (18 mg) with 0.1 M HCl (0.85 mL, 85 mol) and bromophenol blue in acetone/H_2O (1:1, 10 mL) resulted in 3.3 mmol $COO^- g^{-1}$. The particle size-distribution experiments were carried out as described above.

2.2.4. Electrostatic binding of aminodextran-coated iron oxide nanoparticles with 5-aminosalicylic acid as a drug model

5-Aminosalicylic acid (0.33 mg, 0.23 mmol) and magnetic particles (1.0 mg, 3.3 mmol COO^-, 20 equiv) were dissolved in 500 μL H_2O and the solution was shaken for 12 h at room temperature. To purify the product an ultrafiltration device was used for centrifugation and after concentration the sample was washed with H_2O (3 × 2 mL). Size-distribution experiments were carried out as described above.

2.2.5. Measurements

The morphology of the nanoparticles was determined using scanning electron microscopy (SEM, Philips XL 30 scanning electron microscope, Philips, the Netherlands). The particles were coated with gold powder under vacuum before SEM. The crystallinity of the formed nanoparticles was followed with Philips X-ray diffractometer using Cu Kα radiation (λ = 1.5406 Å) as s function of weight percent inorganic component. The Fourier transfer infrared (FT-IR) spectra of the nanoparticles were recorded on Perkin 810 spectrometer in KBr medium at room temperature in the region 4000–450 cm^{-1}. X-ray diffraction patterns and particles size distribution of the aminodextran-coated iron oxide macromolecule were measured by laser light scattering (Malvern Zetasizer ZS, Malvern UK). The samples were examined to determine the mean diameter and size distribution. The samples were prepared by suspending the freeze-dried nanoparticles in 10 mL deionized water (10 g/mL). Drug release from magnetic nanoparticles was carried out using a modified dissolution method. The media was a 0.05 M phosphate buffer solution. Nanoparticle powder (2 mg) was suspended in tubes containing buffer solution of pH 7.4 (10 mL) to simulate physiological pH. The tubes were placed in a shaker bath (Memmert WB14, Germany) at 37 °C.

3. Results and discussion

An important choice of dextran as the molecular backbone was based on practicality and availability. Therefore, active aminodextran molecules have been synthesized in 2-step process (Fig. 1). Fig. 2 shows the SEM of aminodextran-coated iron oxide nanoparticles/5-aminosalicylic acid nanoparticles which were synthesized by chemical reaction. This nanoparticle is very sensitive to temperature. Scanning electron micrography images were obtained from a diluted solution of the nanocomposite particles. The white spots are drug nano particles. The SEM image shows the presence of 5-aminosalicylic acid spherical particles in polyfunctional macromolecule matrix, which are homogeneously distributed throughout the composites, which is also confirmed from ^1H NMR studies.

The ability of the aminodextran-coated iron oxide nanoparticles to form a complex with drugs depends on the nanoparticles and the electrostatic interactions between the nanoparticles and the drug. Therefore, it is possible to manipulate the incorporation process for a given drug by appropriate selection of the nanoparticles

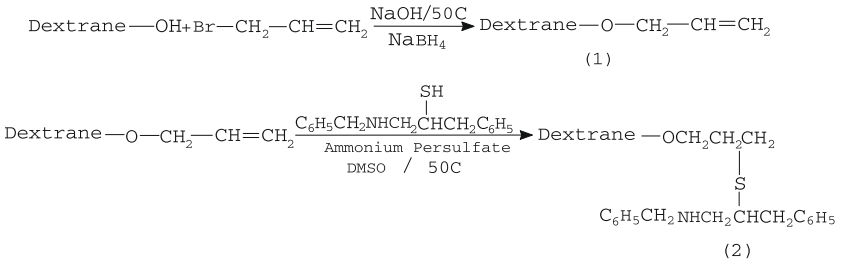

Fig. 1. Covalent attachment of amino groups to dextran hydroxyl groups in 2-step process, which prevents dextran cross-linking. DMSO, dimethyl sulfoxide.

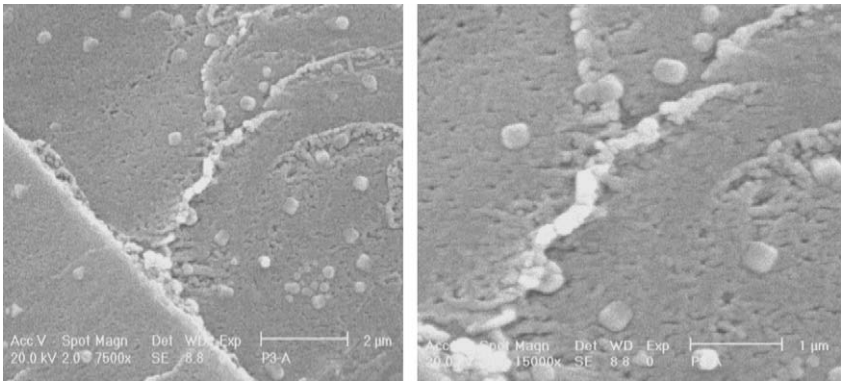

Fig. 2. SEM of aminodextran-coated iron oxide SPIO nanoparticles.

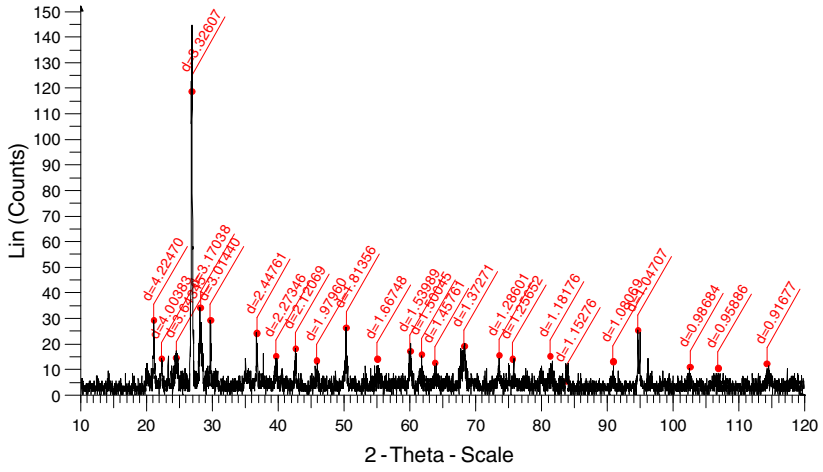

Fig. 3. XRD of aminodextran-coated iron oxide SPIO nanoparticles.

and the surface functionality. One might expect that the 5-aminosalicylic acid with the carboxylic group may form a complex.

Fig. 3 shows X-ray diffraction pattern of aminodextran-coated iron oxide nanoparticles. Diffraction of this macromolecule have a strong peak at about 2θ=26.46°, which is a characteristic peak of aminodextran-coated iron oxide nanoparticles. Studies on XRD patterns of nanoparticles are scarce in the literature. Fig. 4 shows the FT-IR spectrum of aminodextran-coated iron oxide nanoparticles, where the % of transmittance is plotted as a function of wave number (cm^{-1}). The wide peak around 3411 cm^{-1} is attributing to the O–H stretching vibrations of aminodextran. The peaks at 1523 and 1714 cm^{-1} attribute to the COO^- unsymmetrical and symmetrical stretching vibration, respectively. The mean diameter of each conjugate was measured by dynamic light scattering (UPA-150;

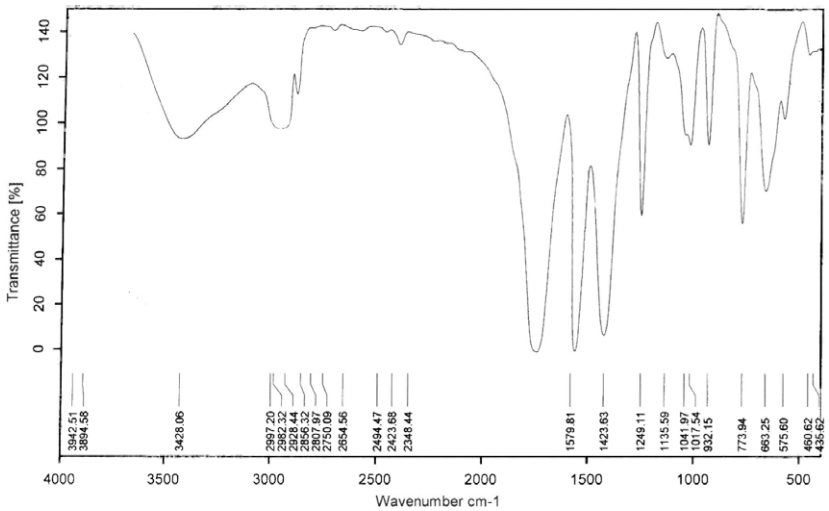

Fig. 4. FT-IR spectrum of aminodextran-coated iron oxide SPIO nanoparticles.

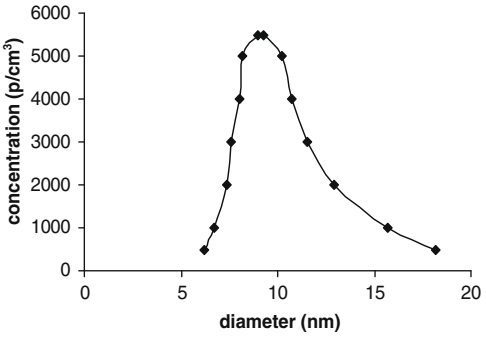

Fig. 5. The particle size distribution of aminodextran-coated iron oxide SPIO/drug conjugate.

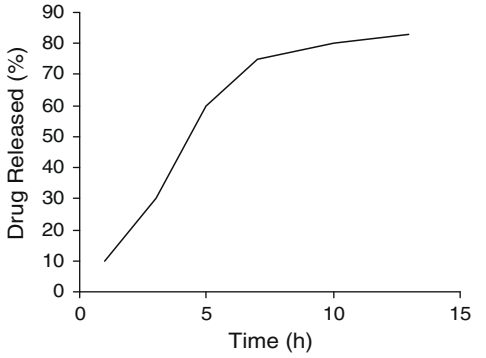

Fig. 6. Drug release (%) to time of aminodextran-coated iron oxide SPIO/drug conjugate.

Honeywell-Microtrac, Clearwater, FL). Each conjugate was assayed for 10 min at a concentration >5 mg/mL of 0.9% saline. The refractor index of each sample was assayed (Fisher Scientific, Santa Clara, CA) and did not deviate from 0.9% saline. Latex particle standards of 3 different sizes gave weight-averaged diameters that were within 5% of their mean diameters (19 ± 1.5, 102 ± 3 and 993 ± 21 nm), which were calibrated by photon correlation spectroscopy or electron microscopy. The analyzer software did not assume a Gaussian size distribution. Mean molecular diameters with SDs were calculated from volume distribution data (Fig. 5). For the learning of nature and size effect of the drug in the drug delivery systems, the drug release behaviour of 5-amniosalicyclic acid as a pharmaceutically active compound has been studied. The concentration of the drug released at selected time intervals was determined by UV spectrophotometry, (λ_{max} = 226 nm), respectively. In order to study the potential application of nanoparticles containing 5-aminosalicylic acid as pharmaceutically active compounds, the drug release behavior of polymers have been studied under physiological conditions (Fig. 6). The concentration of drug in released at selected time intervals was determined by UV spectrophotometry. The decrease of particles size is an important parameter in the diffusion coefficient change. It appears that the degree of drug release polymer depends on their particle size. In the other hand, the chemical structure of the drug too is an important factor in the hydrolytic behavior of polymeric pro-drugs. The high different hydrolysis rate 5-aminosalicylic acid at pH 7.4 can be related to the functional groups along the drug. 5-Aminosalicylic acid contains both amine (basic) and carboxylic acid (acidic) functional groups. This factor ultimately results in an increase in hydrophilicity of 5-aminosalicylic acid at pH 7.4.

The average number of amino groups per dextran was measured in the following manner. The lyophilized dextran conjugate was dissolved in saline, and the amine concentration was measured by the trinitrobenzene sulfonate assay using hexylamine as a standard. The glucose concentration of the same sample was measured by the sulfuric acid method. The amino density was calculated by dividing the amine concentration by the glucose concentration and by multiplying the average number of glucose units per dextran.

4. Conclusions

Aminodextran-coated iron oxide nanoparticles are the first member of a new class of important agents based on macromolecular backbone with a high density of sites for the magnetic resonance imaging (MRI) reporters. This radiopharmaceutical is the first specifically designed anticancer drug carrier. Our long-term goal is to increase the pharmaceutical performance of the MRI technique. The result would be a wider dissemination, beyond academic centers and greater access for patients with cancer or melanoma.

References

Vera, D. R., Buonocore, M. H., Wisner, F. R., Katzberg, R. W., & Stadalnik, R. C. (1995). A molecular receptor-binding contrast for magnetic resonance imagining of the liver. *Academic Radiology, 2*, 497–507.

Vera, D. R., Wisner, E. R., & Stadalnik, R. C. (1997). Sentinel node imaging via a nonparticulate receptor-binding radiotracer. *Journal of Nuclear Medicine, 38*, 530–535.

Morton, D. L., Wen, D. R., & Wong, J. H. (1992). Technical details of intraoperative lymphatic mapping for early stage melanoma. *Archives of Surgery, 127*, 392–399.

Glass, L. F., Messina, J. L., & Cruse, W. (1996). The use of intraoperative radiolymphoscintigraphy for sentinel node diopsy in patients with malignant melanoma. *Dermatologic Surgery, 22*, 715–720.

Gershenwald, J. E., Tseng, C. H., & Thomson, W. (1998). Improved sentinel lymph node localization in patients with primary melanoma with the use of radiolabeled colloid. *Surgery, 124*, 203–210.

Giuliano, A. E., Kirgan, D. M., Guenther, J. M., & Morton, D. L. (1994). Lymphatic mapping and sentinel lymphadenectomy for breast cancer. *Annals of Surgery, 220*, 391–401.

Chipowsky, S., & Lee, Y. C. (1973). Synthesis of 1-thioaldosides having an amino group at the aglycon terminal. *Carbohydrate Research, 31*, 339–346.

Lee, Y. C., Stowell, C. P., & Krantz, M. J. (1976). 2-Imino-2-methoxyethyl-1-thioglycosides: New reagents for attaching sugars to proteins. *Biochemistry, 15*, 3956–3963.

Qu, T., Wang, Y., Zhu, Z., Rusckowski, M., & Hnatowich, D. J. (2001). Different chelators and different peptides together influence the in vitro and mouse in vivo properties of Tc. *Nuclear Medicine Communications, 22*, 203–215.

Shirakami, Y., Mtsumura, Y., Yamamichi, Y., Kurami, M., Ueda, N., & Hazue, M. (1987). Developing of Tc-DTPA-HAS as a new blood pool agent. *Japanese Journal of Nuclear Medicine, 24*, 475–478.

Tomalia, D. A., Baker, H., & Deward, J. (1985). A new class of polymers: Starburst dendritic macromolecules. *Polymer Journal, 17*, 117–132.

Porter, C. J. H. (1997). Drug delivery to the lymphatic system. *Critical Reviews in Therapeutic Drug Carrier, 14*, 333–393.

Nugent, J., & Jain, R. K. (1984). Extravascular diffusion in normal and neoplastic tissues. *Cancer Research, 44*, 234–244.

Thoren, L. (1978). Dextran as a plasma volume substitute. In G. A. Jamieson & T. J. Greenwalt (Eds.), *Blood substitutes and plasma expenders* (pp. 265–282). New York, NY: Alan R. Liss.

Krejcarek, G. E., & Tucker, K. L. (1977). Covalent attachment of chelating groups to macromolecules. *Biochemical and Biophysical Research Communications, 77*, 581–583.

Korosy, F., & Barczai-Martos, M. (1950). Preparation of acetobrome-sugars. *Nature, 165*, 169.

de Belder, D. (1996). Medical application of dextran and its derivatives. In S. Dumitru (Ed.), *Polysaccharides in medical applications* (pp. 505–524). New York, NY: Marcel Dekker.